ELECTRONICS AND ELECTRICAL ENGINEERING
ISSN 1392 – 1215 *2011. No. 4(110)*
ELEKTRONIKA IR ELEKTROTECHNIKA

ELECTRICAL ENGINEERING
T 190
ELEKTROS INŽINERIJA

Computation of Electric Wind Parameters in Direct Current Corona Field

J. Gudzinskas, P. Marciulionis, S. Zebrauskas
Department of Electrical Engineering, Kaunas University of Technology,
Studentų str. 48, LT-51367 Kaunas, Lithuania, phone: +370 37 300268, e-mail: stasys.zebrauskas@ktu.lt

Introduction

Direct current corona discharge is often used in many industry applications to charge small particles and liquid droplets and to control trajectories of their motion. Movement of charges in outer zone of the discharge is complicated due to drag of neutral air molecules. This is the reason of electrohydrodynamic flow rise named as electric wind. Electric wind phenomenon can be used for heat and mass enhancement, in ionic air cleaners etc. [1]. During the last decades many results of experimental and theoretical research are published [2]. Because of high voltage conditions in the discharge gap authors use for experimental research laser-Doppler anemometers, particle image velocimetry systems or hot-wire anemometers [3]. Theoretical research is related to simultaneous analysis of electric field in the electrode system with direct-current corona discharge and air flow field in the system. Analytical study of this complex problem can be performed only for one-dimensional field of coaxial electrode system. Analysis of the complex field in all practical electrode systems, such as wire-to-plate, pin-to-plate etc, is available only by use of numerical methods. Finite-element method (FEM) of characteristics (MoC), boundary element method (BEM) of MoC, FEM-charge simulation method (CSM) and finite-difference method (FDM)-MoC are often used for numerical analysis of the field [2, 3]. Numerical analysis of the electric field of the system can be performed by use of software packages COMSOL or ANSYS [4], air flow field usually is simulated by use of package FLUENT [2]. Numerical study by aid of these packages is related to the use of high-capacity computers. We present there the results of field simulation numerical model based on the FDM in the environment of the package DELPHI suitable to use the domestic personal computer of the usual capacity. Moreover, the generation of computational grid by use the FDM is easier in comparison with FEM.

Numerical modeling of corona field

We present there results of an analysis of electro-hydrodynamic air flow field in the wire-to-plane electrode system suitable to other two-dimensional electrode systems with wire emitting electrodes. Procedure of numerical analysis of the field consists of two stages. The first stage comprises of the numerical solution of the Poisson and charge conservation equations describing the direct-current corona discharge. The results of this stage are the components of Coulomb force in each the node of computational grid. The second stage performs computation of electrohydrodynamic flow field by use of Navier-Stokes and flow continuity equations. We perform an analysis of corona field in polar system of coordinates because of very sharp variation of electric field strength near the zone of ionization on the surface of wire electrode. The view of computational grid for the wire-to-plane electrode system is shown in Fig. 1. Finite-difference approximation of the Poisson equation for irregular polar grid contains potential differences related to distances between central grid node O and neighbouring nodes P, R, Q and S [5, 6]

$$\frac{2V_{\mathrm{P}}}{a_{\mathrm{P}}^2+a_{\mathrm{P}}a_{\mathrm{R}}}+\frac{2V_{\mathrm{R}}}{a_{\mathrm{R}}^2+a_{\mathrm{P}}a_{\mathrm{R}}}+\frac{2V_{\mathrm{Q}}}{a_{\mathrm{Q}}^2+a_{\mathrm{Q}}a_{\mathrm{S}}}+\frac{2V_{\mathrm{S}}}{a_{\mathrm{S}}^2+a_{\mathrm{Q}}a_{\mathrm{S}}}+\frac{a_S V_{\mathrm{Q}}}{r_1(a_{\mathrm{Q}}^2+a_{\mathrm{Q}}a_{\mathrm{S}})}-$$
$$-\frac{a_Q V_{\mathrm{S}}}{r_1(a_{\mathrm{S}}^2+a_{\mathrm{Q}}a_{\mathrm{S}})}-V_{\mathrm{O}}\left(\frac{2}{a_{\mathrm{Q}}a_S}+\frac{2}{a_{\mathrm{R}}a_{\mathrm{P}}}+\frac{a_{\mathrm{S}}^2-a_{\mathrm{Q}}^2}{r_1\left(a_{\mathrm{Q}}a_{\mathrm{S}}^2+a_{\mathrm{S}}a_{\mathrm{Q}}^2\right)}\right)=-\frac{\rho_{\mathrm{O}}}{\varepsilon}. \quad (1)$$

Finite difference approximation of the charge conservation equation has the form

$$\frac{\partial\rho}{\partial r}\cdot\frac{\partial V}{\partial r}+r\frac{\partial\rho}{\partial\varphi}\cdot r\frac{\partial V}{\partial\varphi}=\frac{\rho^2}{\varepsilon}, \quad (2)$$

where partial derivatives of potential are the following:

$$\frac{\partial V}{\partial r}=-\frac{V_{\mathrm{S}}a_{\mathrm{Q}}}{a_{\mathrm{S}}\left(a_{\mathrm{Q}}+a_{\mathrm{S}}\right)}+\frac{V_{\mathrm{Q}}a_{\mathrm{S}}}{a_{\mathrm{Q}}\left(a_{\mathrm{Q}}+a_{\mathrm{S}}\right)}+\frac{V_{\mathrm{O}}\left(a_{\mathrm{Q}}-a_{\mathrm{S}}\right)}{a_{\mathrm{Q}}a_{\mathrm{S}}}, \quad (3)$$

$$\frac{r\partial V}{\partial \varphi} = -\frac{V_{\mathrm{P}} a_{\mathrm{R}}}{a_{\mathrm{P}}\left(a_{\mathrm{P}} + a_{\mathrm{R}}\right)} + \frac{V_{\mathrm{R}} a_{\mathrm{P}}}{a_{\mathrm{R}}\left(a_{\mathrm{P}} + a_{\mathrm{R}}\right)} + \frac{V_{\mathrm{O}}\left(a_{\mathrm{P}} - a_{\mathrm{R}}\right)}{a_{\mathrm{P}} a_{\mathrm{R}}} \quad (4)$$

and the partial derivatives of the charge density are of the form:

$$\frac{\partial \rho}{\partial r} = \frac{\rho_{\mathrm{Q}} a_{\mathrm{S}}}{a_{\mathrm{Q}}\left(a_{\mathrm{Q}} + a_{\mathrm{S}}\right)} - \frac{\rho_{\mathrm{S}} a_{\mathrm{Q}}}{a_{\mathrm{S}}\left(a_{\mathrm{Q}} + a_{\mathrm{S}}\right)} + \frac{\rho_{\mathrm{O}}\left(a_{\mathrm{Q}} - a_{\mathrm{S}}\right)}{a_{\mathrm{Q}} a_{\mathrm{S}}}, \quad (5)$$

$$\frac{r\partial \rho}{\partial \varphi} = -\frac{\rho_{\mathrm{P}} a_{\mathrm{R}}}{a_{\mathrm{P}}\left(a_{\mathrm{P}} + a_{\mathrm{R}}\right)} + \frac{\rho_{\mathrm{R}} a_{\mathrm{P}}}{a_{\mathrm{R}}\left(a_{\mathrm{P}} + a_{\mathrm{R}}\right)} - \frac{\rho_{\mathrm{O}}\left(a_{\mathrm{P}} - a_{\mathrm{R}}\right)}{a_{\mathrm{P}} a_{\mathrm{R}}}. \quad (6)$$

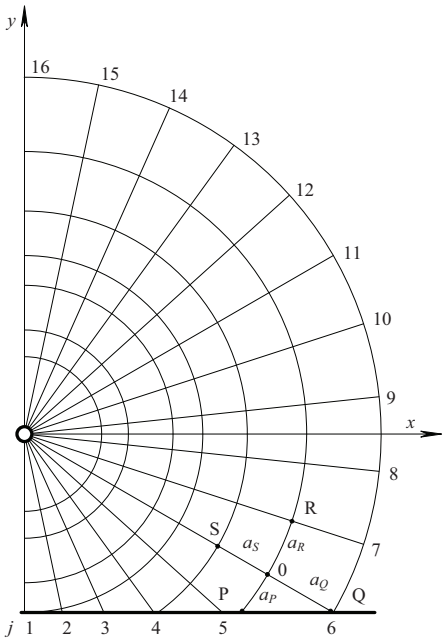

Fig. 1. Polar grid for wire-to-plane electrodes if m = 15

Components of electric field strength are the first derivatives of potential (for irregular polar grid):

$$E_r = -\frac{\partial V}{\partial r} = \frac{V_{\mathrm{S}} a_{\mathrm{Q}}}{a_{\mathrm{S}}^2 + a_{\mathrm{Q}} a_{\mathrm{S}}} - \frac{V_{\mathrm{Q}} a_{\mathrm{S}}}{a_{\mathrm{Q}}^2 + a_{\mathrm{Q}} a_{\mathrm{S}}} + \frac{V_{\mathrm{O}}\left(a_{\mathrm{S}}^2 - a_{\mathrm{Q}}^2\right)}{a_{\mathrm{Q}}^2 a_{\mathrm{S}} + a_{\mathrm{Q}} a_{\mathrm{S}}^2}, \quad (7)$$

$$E_\varphi = -\frac{\partial V}{r\partial r} = \frac{V_{\mathrm{P}} a_{\mathrm{R}}}{a_{\mathrm{P}}^2 + a_{\mathrm{R}} a_{\mathrm{P}}} - \frac{V_{\mathrm{R}} a_{\mathrm{P}}}{a_{\mathrm{R}}^2 + a_{\mathrm{R}} a_{\mathrm{P}}} + \frac{V_{\mathrm{O}}\left(a_{\mathrm{P}}^2 - a_{\mathrm{R}}^2\right)}{a_{\mathrm{R}}^2 a_{\mathrm{P}} + a_{\mathrm{P}} a_{\mathrm{R}}^2}. \quad (8)$$

Boundary conditions for the problem solving are the following. Potential of the wire is equal to the given voltage U, potential of the plane electrode is equal to 0. The field strength on the surface of emitting electrode is constant, if $U \geq U_0$ in accordance with the Kaptzov's assumption [1]. U_0 is the corona onset voltage. Charge density on the surface of the wire $\rho(r_0)$ is increased from the value $\rho = 0$ by the step $\delta\rho$ to the value corresponding the field strength condition $E(r_0) = E_0$. Computation procedure is shown in Fig. 2.

At the beginning wire potential is increased from 0 until it reaches given voltage U. If the field strength $E(r_0) < E_0$ Laplace's equation is being solved, in the other case we find the solution of Poisson's equation. We solve this equation and the charge conservation equation until two conditions $E(r_0) = E_0$ and $V(r_0) = U$ are satisfied. At the end we find field strength components E_r and E_φ by use the equations (7), (8).

Results of numerical modelling of direct-current corona field are given in Fig. 3 by presenting computed and experimental current-voltage characteristics. Parameters of wire-to-plane electrode system are the following: radius of the wire r_0 = 0,05 mm, spacing between the wire and the plane electrode h = 12,0 mm, range of voltage variation U = 4,5–10,0 kV, negative corona ion mobility k = 2,20 cm^2/V·s. Characteristic parameter of polar grid m = 15, corresponding to the central angle between neighbour radial lines φ_0 = 12° (0,209 rad). Number of nodes in computational area shown in Fig. 1 is 518. The law of changing of coordinate r is the following

$$r_i = r_0 \cdot \left(1 + (\pi / m)\right)^{i-1}. \quad (9)$$

The value of linear discharge current density is defined as an integral of current density on side-on surface of the wire

$$I_0 = (1/l) \int_{S_0} \boldsymbol{J} \cdot \mathrm{d}\boldsymbol{S} = S_0 / l \sum_{j=1}^{m} \left[J(j-1) + J(j)\right], \quad (10)$$

where $\boldsymbol{J}$ is current density

$$\boldsymbol{J} = \rho(r_0) \cdot k \cdot \boldsymbol{E}(r_0) \quad (11)$$

and S_0 is the side-on surface of the wire of unit length.

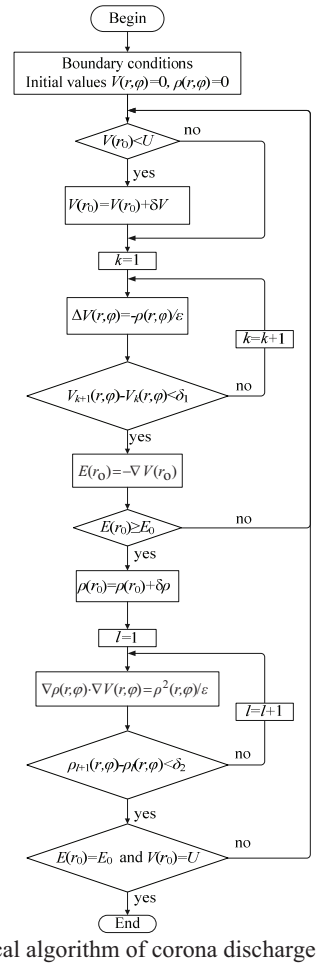

Fig. 2. Numerical algorithm of corona discharge field analysis

Maximum difference between numerical and experimental values of linear current density shown in Fig. 3 corresponding to the voltage value U = 7,0 kV is 150 μA/m. The laws of numerical and experimental current variations corresponding to the rising voltage values are the similar.

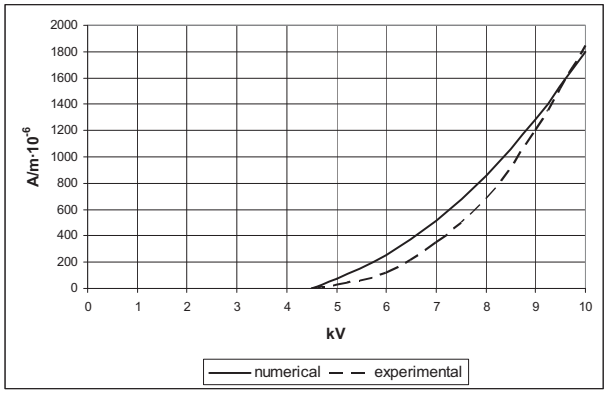

Fig. 3. Current-voltage characteristic

Numerical analysis of electrohydrodynamic air flow

Incompressible and viscous air flow induced by Coulomb force determined as the production of electric charge density and field strength of the discharge is governed by the system of equations comprising of the Navier-Stokes and the flow continuity equations (for steady-state conditions). The area of cross section of emitting electrode with the zone of ionization is negligible in comparison with the overall computation area of the field and the cross section of the wire can be assumed as a point. Therefore the grid in Cartesian system of coordinates can be used for computation of velocity components.

Finite-difference approximation of the Navier-Stokes and the flow continuity equations for this system of coordinates contains the Coulomb force components F_x, F_y and the flow velocity components w_x, w_y:

$$w_{x\mathrm{C}}^{(\tau+1)} = \left(\frac{F_x}{\rho_v} + \nu\left(\frac{w_{x\mathrm{P}}}{a^2} + \frac{w_{x\mathrm{R}}}{a^2} + \frac{w_{x\mathrm{Q}}}{a^2} + \frac{w_{x\mathrm{S}}}{a^2} - \frac{4w_{x\mathrm{C}}}{a^2}\right) - w_{xO}\left(\frac{w_{x\mathrm{C}} - w_{x\mathrm{P}}}{a}\right) - w_{y\mathrm{O}}\left(\frac{w_{x\mathrm{C}} - w_{x\mathrm{S}}}{a}\right)\right)\cdot\Delta\tau + w_{x\mathrm{C}}^{(\tau)}, \quad (12)$$

$$w_{y\mathrm{C}}^{(\tau+1)} = \left(a_y + \frac{F_y}{\rho_v} + \nu\left(\frac{w_{y\mathrm{P}}}{a^2} + \frac{w_{y\mathrm{R}}}{a^2} + \frac{w_{y\mathrm{Q}}}{a^2} + \frac{w_{y\mathrm{S}}}{a^2} - \frac{4w_{y\mathrm{O}}}{a^2}\right) - w_{xO}\left(\frac{w_{y\mathrm{C}} - w_{y\mathrm{P}}}{a}\right) - w_{y\mathrm{O}}\left(\frac{w_{y\mathrm{C}} - w_{y\mathrm{S}}}{a}\right)\right)\cdot\Delta\tau + w_{y\mathrm{C}}^{(\tau)}, \quad (13)$$

$$\frac{w_{y\mathrm{C}} - w_{y\mathrm{S}}}{a} - \frac{w_{x\mathrm{P}} - w_{x\mathrm{R}}}{a} = 0. \quad (14)$$

There $w_{x\mathrm{C}}^{(\tau+1)}$ is the velocity x component value of new iteration, $w_{x\mathrm{C}}^{(\tau)}$ is the value of previous iteration, $w_{x\mathrm{P}}$, $w_{x\mathrm{R}}$, $w_{x\mathrm{S}}$, $w_{x\mathrm{Q}}$ are the x components of velocities in the neighbour nodes, $w_{x\mathrm{O}}$ is the x axis component of average velocity in the square (Fig. 4), $\Delta\tau$ - variation of time between iterations, a – distance between nodes, regular in all the grid.

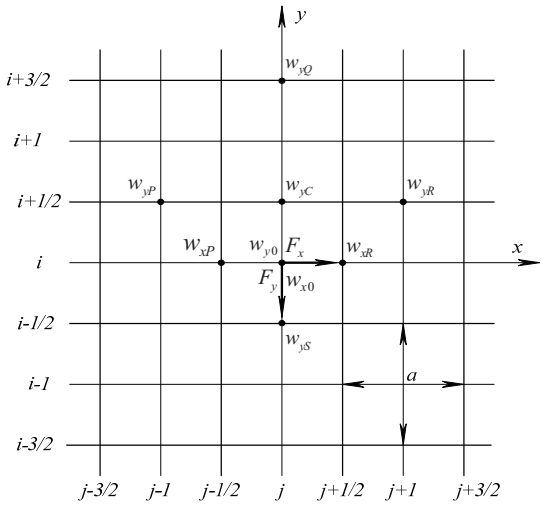

Fig. 4. Computational grid with square elements

Computation of air flow field is performed in accordance with boundary conditions. At the beginning of computation, for $\tau = 0$, air velocities in all the area $w = 0$. We assume that air is incompressible, therefore air density ρ_v= const. Coefficient of kinematic viscosity is assumed as constant $\nu = 1{,}507\cdot10^5$ m^2/s for t = 20 °C and $p = 1{,}033\cdot10^5$ Pa. Velocity component $w_x = 0$ in all points of y axis ($x = 0$) due to the symmetry of the field. Components $w_x = 0$ and $w_y = 0$ on the surface of the plane electrode ($x = -h$) because of stillness of the air at the boundary. The condition for free space boundary is constructed by use of the assumption that the velocity derivatives in the inner point near the boundary and the outer one are the same for the determined value of i or j (Fig. 4).

Procedure of electrohydrodynamic air flow field computation is shown in Fig. 5. Iterative successively computation by equations (12), (13) and (14) is repeated until stationary conditions are established.

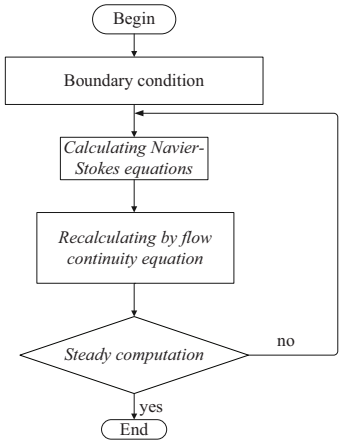

Fig. 5. Computation scheme for numerical analysis of air flow

Visual representation of air flow velocities is given by vectors in Fig. 6. The length of each vector is proportional to modulus of velocity and the angle is proportional to the meaning of function arctan(w_y/w_x), where w_x and w_y are the components of velocity.

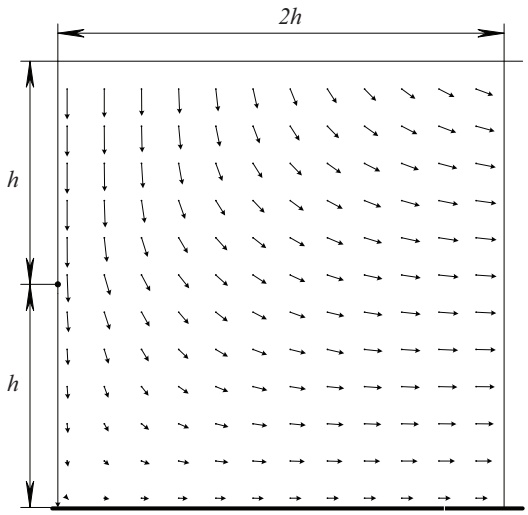

Fig. 6. Electrohydrodynamic air flow distribution in the electrode system for h = 12 mm

Velocity y-component gains maximum values of ~4 m/s on the axis of symmetry and near it above the wire. That component diminishes to 0 on the approach to the plane electrode. Velocity x-component increases with receding from the axis of symmetry.

Experimental test of analysis is performed by comparison of numerical results with the ones of measurement by use of hot-wire anemometer DO 9847K. Anemometer probe placed near the discharge electrode distorts not only the electric field but also the air flow field. Therefore comparison of the results is only qualitative. Numerical value of velocity at the point x = 6 cm near the surface of plane electrode is 1,57 m/s, the measured value is 1,02 m/s. The difference between the results is 35 %. Such a disagreement is determined by the field distortion and by the assumptions of modeling.

Conclusions

Two-dimensional numerical model of direct current corona field analysis in wire-to-plane electrode system is based upon the finite-difference method in polar system of coordinates.

Results of corona field modeling are tested by comparison of the numerical and experimental current-voltage characteristics. Maximum difference of discharge current values at U = 7,0 kV is 150 μA/m.

Numerical model of electrohydrodynamic flow field analysis is based upon the finite-difference method in Cartesian system of coordinates.

Numerical value of velocity in the point near the plane electrode at x = 6,0 cm differs from value measured by means of hot-wire anemometer by 35 %.

References

1. **Zhao L., Adamiak K.** EHD Flow in Air Produced by Electric Corona Discharge in Pin–Plate Configuration // Journal of Electrostatics, 2005. – Vol. 63. – No. 3–4. – P. 337–350.
2. **Farnoosh N., Adamiak K., Castle G.S.P.** 3–D Numerical Analysis of EHD Turbulent Flow and Mono–disperse Charged Particle Transport and Collection in a Wire–plate ESP // Journal of Electrostatics, 2010. – Vol. 68. – No. 6. – P. 513–522.
3. **Morozionkov J.,Virbalis J. A.** Investigation of Electric Reactor Magnetic Field using Finite Element Method // Electronics and Electrical Engineering. – Kaunas: Technologija, 2008. – No. 5(85) – P. 9–12.
4. **Morozionkov J., Virbalis J. A.** Shielding of Electric Reactor Magnetic Field // Electronics and Electrical Engineering. – Kaunas: Technologija, 2009. – No 8(96). – P. 13–18.
5. **Marciulionis P., Zebrauskas S.** Equations of DC Corona Electric Wind Velocities // Electronics and Electrical Engineering. – Kaunas: Technologija, 2007. – No 8(80). – P. 73–76.
6. **Marčiulionis P., Zebrauskas S.** Numerical Analysis of Spatial Force Components in Direct Current Corona Field // Electronics and Electrical Engineering. – Kaunas: Technologija, 2009. No. 8(96). – P. 3–8.

Received 2011 03 18

J. Gudzinskas, P. Marciulionis, S. Zebrauskas. Computation of Electric Wind Parameters in Direct Current Corona Field // Electronics and Electrical Engineering. – Kaunas: Technologija, 2011. – No. 4(110). – P. 3–6.

Digital model for analysis of two-dimensional direct current corona field and induced electrohydrodynamic air flow field in wire-to-plane electrode system is discussed. Finite-difference method in polar coordinate system is used for corona field computation. Results of computation of corona field are checked by comparison of digital and experimental data of current-voltage characteristics. Maximum difference of these values of linear current density is 150 μA/m corresponding to the voltage value of 7 kV. The digital model of EHD air flow field consists of finite-difference approximation of the Navier-Stokes equation and the continuity equation in Cartesian coordinates. Check of digital velocity values by comparison of these values with the experimental ones is only qualitative because of the distortion of corona field and air flow field by the probe of hot-wire anemometer. Ill. 6, bibl. 6 (in English; abstracts in English and Lithuanian).

J. Gudzinskas, P. Marčiulionis, S. Žebrauskas. Vienpolio vainikinio išlydžio elektrinio vėjo parametrų skaičiavimas // Elektronika ir elektrotechnika. – Kaunas: Technologija, 2011. – Nr. 4(110). – P. 3–6.

Analizuojamas elektrodų sistemos „laidas šalia plokštumos“ dvimačio vienpolio vainikinio išlydžio elektrinio lauko ir jo sukelto oro tekėjimo lauko analizės skaitinis modelis. Vainikinio išlydžio elektrinis laukas skaičiuojamas baigtinių skirtumų metodu polinėje koordinačių sistemoje. Nustatyta, kad didžiausias ilginio srovės tankio skaitinių ir eksperimentinių verčių skirtumas yra 150 μA/m, kai išlydžio įtampa yra 7 kV. Oro tekėjimo lauko lygčių sistemos skaitinį modelį sudaro Navier ir Stokeso, taip pat tolydumo lygties skirtuminė aproksimacija Dekarto koordinačių sistemoje. Skaitinės greičių vertės palygintos su eksperimentinėmis tik kokybiškai, nes termoanemometro jutiklis iškraipo lauką. Il. 6, bibl. 6 (anglų kalba; santraukos anglų ir lietuvių k.).